

AD _____

Award Number: DAMD17-02-1-0039

TITLE: Investigation of SNARE-Mediated Membrane Trafficking in
Prostate Cancer Cells

PRINCIPAL INVESTIGATOR: Xin Li, M.D., Ph.D.

CONTRACTING ORGANIZATION: The Cleveland Clinic Foundation
Cleveland, Ohio 44195

REPORT DATE: February 2003

TYPE OF REPORT: Annual Summary

PREPARED FOR: U.S. Army Medical Research and Materiel Command
Fort Detrick, Maryland 21702-5012

DISTRIBUTION STATEMENT: Approved for Public Release;
Distribution Unlimited

The views, opinions and/or findings contained in this report are those of the author(s) and should not be construed as an official Department of the Army position, policy or decision unless so designated by other documentation.

20030702 038

REPORT DOCUMENTATION PAGE

Form Approved
OMB No. 074-0188

Public reporting burden for this collection of information is estimated to average 1 hour per response, including the time for reviewing instructions, searching existing data sources, gathering and maintaining the data needed, and completing and reviewing this collection of information. Send comments regarding this burden estimate or any other aspect of this collection of information, including suggestions for reducing this burden to Washington Headquarters Services, Directorate for Information Operations and Reports, 1215 Jefferson Davis Highway, Suite 1204, Arlington, VA 22202-4302, and to the Office of Management and Budget, Paperwork Reduction Project (0704-0188), Washington, DC 20503

1. AGENCY USE ONLY (Leave blank)		2. REPORT DATE February 2003	3. REPORT TYPE AND DATES COVERED Annual Summary (1 Feb 02 - 31 Jan 03)	
4. TITLE AND SUBTITLE Investigation of SNARE-Mediated Membrane Trafficking in Prostate Cancer Cells			5. FUNDING NUMBERS DAMD17-02-1-0039	
6. AUTHOR(S) Xin Li, M.D., Ph.D.				
7. PERFORMING ORGANIZATION NAME(S) AND ADDRESS(ES) The Cleveland Clinic Foundation Cleveland, Ohio 44195 E-mail: lix2@ccf.org			8. PERFORMING ORGANIZATION REPORT NUMBER	
9. SPONSORING / MONITORING AGENCY NAME(S) AND ADDRESS(ES) U.S. Army Medical Research and Materiel Command Fort Detrick, Maryland 21702-5012			10. SPONSORING / MONITORING AGENCY REPORT NUMBER	
11. SUPPLEMENTARY NOTES Original contains color plates: All DTIC reproductions will be in black and white.				
12a. DISTRIBUTION / AVAILABILITY STATEMENT Approved for Public Release; Distribution Unlimited			12b. DISTRIBUTION CODE	
13. Abstract (Maximum 200 Words) (abstract should contain no proprietary or confidential information) The specific purposes of this project are to investigate how the expression and localization of membrane SNAREs in prostate carcinomas, and what the relationship to the degree of malignancy and metastasis. 15 transgenic mice of prostate cancer (Tramp) with different stages of carcinogenesis, and 5 cases of human prostatic carcinomas were used. Paraffin sections were immuno-stained with anti-t-SNARE antibodies, syntaxin 3 and syntaxin 4. The localizations of t-SNAREs were observed with a confocal microscope. Cell polarity was preserved in most prostatic lesions both in Tramp mice and human prostatic cancers as shown by basolateral E-cadherin, except one metastatic lesion in the kidney of one Tramp mouse. Down-regulation of syntaxin 3 was observed in 7 of 15 tramp mice, and in 4 of 5 human prostate cancers. This is correlated with the low degrees of differentiation, down-expression of E-cadherin and p27. But the intracellular localization of syntaxin 3 and 4 was only observed in the metastatic lesions, suggesting that down-regulation and mislocalization of t-SNARE play a role in progression of prostate cancer.				
14. SUBJECT TERMS: SNARE, cell polarity, prostate cancer			15. NUMBER OF PAGES 20	
			16. PRICE CODE	
17. SECURITY CLASSIFICATION OF REPORT Unclassified	18. SECURITY CLASSIFICATION OF THIS PAGE Unclassified	19. SECURITY CLASSIFICATION OF ABSTRACT Unclassified	20. LIMITATION OF ABSTRACT Unlimited	

Table of Contents

Cover.....	1
SF 298.....	2
Table of Contents.....	3
Introduction.....	4
Body.....	4
Reportable Outcomes.....	6
Appendices.....	8

Report for “Investigation of SNARE-mediated Membrane Trafficking in Prostate Cancer Cells” -DAMD17-02-1-0039

The first part of this project is to investigate the expression and localization of SNARE proteins in human prostate cancer tissues and transgenic mouse of prostate cancers (Tramp). During the past year, 15 Tramp mice were obtained. By histology, these mice showed different stages of prostatic carcinogenesis, with a metastatic lesion in the kidney in one mouse, and 6 mice accompanying tumors in the seminal vesicle. 5 cases of human prostatic carcinomas were obtained from the Department of Surgical Pathology, Cleveland Clinic Foundation. All of these cases were moderately differentiated adenocarcinomas without metastasis, which is the most common type of prostate cancer. The human prostatic cancer cell line LNCap was also used.

Major Findings

- **Plasma membrane t-SNAREs (i.e. syntaxin 3 and syntaxin 4) are expressed in human and mouse prostate gland**

Plasma membrane t-SNAREs, i. e. syntaxin 3 and syntaxin 4 in this study, which were found to mislocalize to the intracellular vacuoles upon the loss of cell polarity in our previous study, were shown to be expressed in the prostate gland and prostate cancer in mouse and human by immunofluorescence (Fig. 1) and Western blot (Fig. 2). Syntaxin 3 is localized to the apical plasma membrane, and syntaxin 4 is localized to the basolateral plasma membrane by confocal microscopy.



Fig. 1 Localization of syntaxin3 (1A) and 4 (1B) in normal mouse prostate gland and human prostate gland (1C). Syntaxin 3 and 4 are localized to the apical and basolateral membrane of normal prostate epithelial cells, respectively. Syntaxin 3 (1A and 1C) and 4 (1B) are labeled with green color, whereas E-cadherin (1A and 1C) and p27 (1B) are labeled with red color.

Expression of syntaxins 3 and 4 was also shown by Western blot analysis using the human prostate cancer cell line, LNCap cells (Fig. 2). The expression level of syntaxin 3 is higher than that of syntaxin 4.

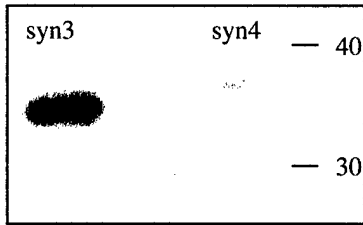


Fig. 2. Western blot analysis of syntaxins in LNCap cells. Total lysate of LNCap cells was run on a 10% SDS gel, and immunoblotted with anti-syntaxin 3 (left lane), or syntaxin 4 (right lane) antibody.

- **Syntaxin3 is down-regulated in tumor cells in Tramp mice and in human prostate cancers.**

Our preliminary results showed mistargeting of syntaxin 3 and 4 in renal cell carcinoma, and down-regulation of syntaxin 3 in Tramp mice. Prostate tissues from 15 Tramp mice and 5 human prostate cancers were investigated to investigate whether this is a common feature of prostate cancer, and its relationship to the cell polarity, tumor differentiation and proliferation. Cell polarity was evaluated by the basolateral marker E-cadherin. The cell proliferative status was estimated by the cell cycle protein p27, which is a negative regulator of cell proliferation. Syntaxin 3 was found to be down-regulated in 7 of 15 Tramp mice, and in 4 of 5 human prostate cancers (Fig. 3). But this down-regulation was only observed in the poorly-differentiated lesions, not in the prostatic intraepithelial neoplasia (PIN). The same phenomenon was not obvious in the expression of syntaxin4 (data not shown).

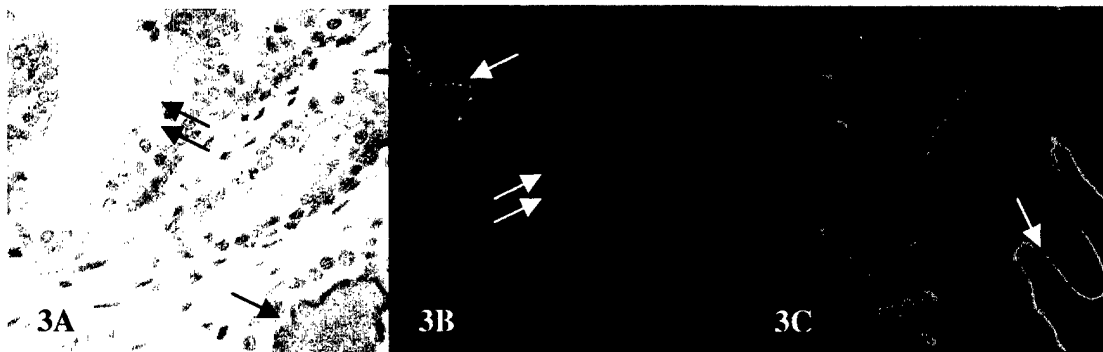


Fig.3 Expression of syntaxin 3 in human prostate cancer (3A), and Tramp mice (3B and 3C). Lower expression of syntaxin3 was detected in the poorly-differentiated lesions of prostate cancer in human and Tramp mice (double arrow in 3A and 3B), but not in the prostatic intraepithelial neoplasia (PIN) (arrow in 3C) compared to well-differentiated acinus (arrow in 3A and 3B). 3A immunoreaction was visualized by DAB not by the fluorescence. The nuclei were counterstained by heamatoxylin.

- **Syntaxin 3 and 4 are mislocalized to intracellular vesicles in metastatic prostate cancer cells**

One Tramp mouse exhibited a metastatic cancer in the right kidney (the left kidney was normal). The histology showed similar structures to the primary carcinomas in the prostate, but with less-differentiation (Fig. 4A and B). The localization of syntaxin 3 and 4 was in intracellular structures instead of plasma membrane. The same localization was found in a human prostatic cancer cell line (originated from metastatic cancer to the lymph node), LNCap cells (Fig.5A and 5B). In contrast, intracellular localization of syntaxin 3 or 4 was not detectable in human prostate cancer. The likely reason is that the available cases used were moderately differentiated adenocarcinomas, which still retain the cell polarity, as shown by basolateral E-cadherin, although we did detect the down-regulated syntaxin 3 and E-cadherin. This suggests that the intracellular localization of syntaxin 3 is related to the complete loss of cell polarity. More aggressive, poorly-differentiated human prostate cancers or metastatic lesions will be used to confirm this.

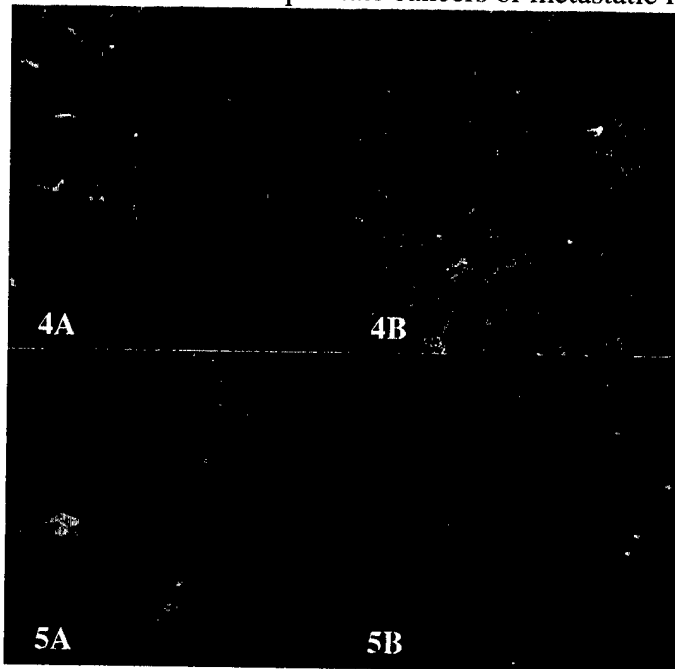


Fig. 4. Localization of syntaxin 3 (4A) and 4 (4B) in the metastatic cancer of Tramp mouse in the kidney. Syntaxin 3 and 4 were found to be intracellular (labeled with green color). E-cadherin (4A) and p27 (4B) were labeled with red color

Fig. 5 Localization of syntaxin 3 (5A) and 4 (5B) in LNCap cells. Syntaxin 3 and 4 are intracellularly stained (green color)

Overall, our results suggest that down-regulation and mislocalization of t-SNARE proteins (e. g. syntaxin 3 and 4) plays a role in the progression of prostate cancer.

Scientific training and papers published under the support of this award

During this study, I have had a great opportunity to collaborate with many scientists who work in the field of prostate cancer, especially the researchers in Dr. Warren Heston's laboratory at the Department of Cancer Biology of the Cleveland Clinic. I learned how to dissect the mouse prostate, and to identify the histological structures of different lobes of the prostate. I attend the monthly research updates on the urological research in the Cleveland Clinic Foundation, communicate the ideas on the research of prostate cancer. Last year I attended the Cell Biology Retreat between the Cleveland Clinic Foundation and Case Western Reserve University, and the annual meeting of American Society of Cell Biology in San Francisco. One first-author paper (*American Journal of Physiology* 283: F1111—F1122 see attached) was published under the support of this award which

lays the groundwork for our investigation of syntaxins in the prostate and prostate cancer. This paper describes our detailed analysis of syntaxin expression and subcellular localization in epithelial cell types along the renal tubule. Renal epithelial cells are now by far the best characterized epithelial system with respect to the SNARE membrane fusion machinery and will serve as a reference standard for our work on the prostate epithelium.

Altogether four papers were authored or co-authored as follows:

Li, X., Low, S.H., Miura, M. and Weimbs, T. (2002)

Differential SNARE Expression and Localization in Renal Epithelial Cells suggests mechanism for establishment of distinct trafficking phenotypes.

American Journal of Physiology 283: F1111–F1122

Low, S.H., Marmorstein, L.Y, Miura, M., **Li, X.**, Kudo, N., Marmorstein, A.D. and Weimbs, T. (2002)

Retinal pigment epithelial cells exhibit unique expression and localization of plasma membrane syntaxins which may contribute to their trafficking phenotype.

Journal of Cell Science 115, 4545-4553

Kreitzer, G., Schmoranzer, J., Low, S.H., **Li, X.**, Gan, Y., Weimbs, T., Simon, S.M. and Rodriguez-Boulan, E. (2003)

Three-dimensional Analysis of Post-Golgi Carrier Exocytosis in Epithelial Cells.

Nature Cell Biology 5, 126-136

Weimbs, T., Low, S.H. and **Li, X.** (2003)

SNAREs and epithelial cells

Methods: A Companion to Methods in Enzymology (in press)

Appendix

SNARE expression and localization in renal epithelial cells suggest mechanism for variability of trafficking phenotypes

XIN LI, SENG HUI LOW, MASUMI MIURA, AND THOMAS WEIMBS
*Department of Cell Biology, Lerner Research Institute, and Urological
Institute, The Cleveland Clinic, Cleveland, Ohio 44195*

Received 22 May 2002; accepted in final form 18 June 2002

Li, Xin, Seng Hui Low, Masumi Miura, and Thomas Weimbs. SNARE expression and localization in renal epithelial cells suggest mechanism for variability of trafficking phenotypes. *Am J Physiol Renal Physiol* 283: F1111–F1122, 2002; 10.1152/ajprenal.00185.2002.—The apical- and basolateral-specific distribution of target soluble *N*-ethylmaleimide-sensitive factor attachment protein receptors (t-SNAREs) of the syntaxin family appear to be critical for polarity in epithelial cells. To test whether differential SNARE expression and/or subcellular localization may contribute to the known diversity of trafficking phenotypes of epithelial cell types *in vivo*, we have investigated the distribution of syntaxins 2, 3, and 4 in epithelial cells along the renal tubule. Syntaxins 3 and 4 are restricted to the apical and basolateral domains, respectively, in all cell types, indicating that their mutually exclusive localizations are important for cell polarity. The expression level of syntaxin 3 is highly variable, depending on the cell type, suggesting that it is regulated in concert with the cellular requirement for apical exocytic pathways. While syntaxin 4 localizes all along the basal and lateral plasma membrane domains *in vivo*, it is restricted to the lateral membrane in Madin-Darby canine kidney (MDCK) cells in two-dimensional monolayer culture. When cultured as cysts in collagen, however, MDCK cells target syntaxin 4 correctly to the basal and lateral membranes. Unexpectedly, the polarity of syntaxin 2 is inverted between different tubule cell types, suggesting a role in establishing plasticity of targeting. The vesicle-associated (v)-SNARE endobrevin is highly expressed in intercalated cells and colocalizes with the H⁺-ATPase in α - but not β -intercalated cells, suggesting its involvement in H⁺-ATPase trafficking in the former cell type. These results suggest that epithelial membrane trafficking phenotypes *in vivo* are highly variable and that different cell types express or localize SNARE proteins differentially as a mechanism to achieve this variability.

syntaxin; endobrevin; membrane traffic; cell polarity; membrane fusion

THE VAST MAJORITY OF HUMAN cell types are polarized, i.e., they exhibit asymmetry, which is essential to their function. This includes epithelial cells, which form barriers between the outside world and the underlying basement membrane and connective tissue and make up most major human organs. Establishment and maintenance of epithelial cell polarity depend on the

precise targeting of proteins to the apical and basolateral plasma membrane domains using vesicular transport pathways (41, 44). The underlying mechanisms of polarized trafficking in epithelial cells have been intensively studied *in vitro* using model cell lines, most frequently in the Madin-Darby canine kidney (MDCK) cell line derived from the distal renal tubule (62).

The soluble *N*-ethylmaleimide-sensitive factor attachment protein receptor (SNARE) membrane fusion machinery is essential for all membrane trafficking pathways investigated to date (10, 24). Target (t)-SNAREs of the syntaxin family generally localize to distinct compartments and organelles, where they mediate the fusion of specific incoming trafficking pathways. Membrane fusion can only occur with matching combinations of vesicle-associated (v)- and t-SNAREs (38, 56), suggesting that SNAREs contribute to the specificity of membrane traffic.

In MDCK cells, syntaxins 3 and 4 are mutually exclusively localized to the apical and basolateral plasma membrane, respectively (30). Syntaxin 3 is involved in apical recycling and in biosynthetic traffic from the *trans*-Golgi network (TGN) to the apical surface (31). In contrast, syntaxin 4 is involved in TGN-to-basolateral trafficking (26). In addition, MDCK cells express syntaxins 2 and 11, the functions of which have remained unknown, and both of which are localized to the plasma membrane in a nonpolarized fashion (30, 32). These results suggest that the correct localization of syntaxins is critical for the fidelity of polarized membrane traffic in epithelial cells.

Higher animal organisms consist of a multitude of epithelial cell types, each of which has specific functions. They vary not only in their proteome of plasma membrane proteins but also in the way they sort and target them to their final destination. Identical proteins can be localized to opposite surfaces in different epithelial cell types. A classic example is the H⁺-ATPase, which is apically localized in α -intercalated cells of the renal distal tubule, whereas it is basolateral in β -intercalated cells (1, 7). The final polarity of a given protein may also be identical between two cell types, but the route by which the proteins reach their

Address for reprint requests and other correspondence: T. Weimbs, Dept. of Cell Biology, Lerner Research Institute, NC10, The Cleveland Clinic, 9500 Euclid Ave., Cleveland, OH 44195 (E-mail: weimbst@lerner.ccf.org).

The costs of publication of this article were defrayed in part by the payment of page charges. The article must therefore be hereby marked "advertisement" in accordance with 18 U.S.C. Section 1734 solely to indicate this fact.

surface differs. For example, MDCK cells target almost all newly synthesized apical proteins (including the influenza virus hemagglutinin) directly from the TGN to the apical surface. In contrast, the retinal pigment epithelium targets the influenza virus hemagglutinin to the apical plasma membrane indirectly by transcytosis via the basolateral domain (4). Hepatocytes are an extreme case and transport virtually all apical proteins by transcytosis (23). The epithelial sorting phenotype can also change during the development of a polarized monolayer (66). Therefore, great variability exists in the protein-targeting phenotypes among epithelial cell types.

It is unclear whether results obtained from MDCK cells are necessarily valid for all epithelial cell types *in vivo*. Moreover, it is unknown how the observed differences in targeting phenotypes between epithelial cell types are achieved mechanistically. We sought to investigate whether differences in the expression and/or subcellular localization of syntaxins may be part of this mechanism. We tested this by investigating syntaxins in epithelial cells along the renal tubule. There are 14 recognizably different epithelial cell types in the kidney (1), which play specific roles such as absorption of proteins and the maintenance of water, ions, and acid-base balance. Differences in membrane trafficking phenotypes between renal epithelial cell types are well known (1, 8, 9). MDCK cells are likely derived from the collecting duct (39), but they also have characteristics of other tubule segments (9). Investigating SNAREs along the renal tubule makes it possible to compare different epithelial cell types side by side and to relate results to the most widely used model system, MDCK cells.

Here, we report similarities and differences between renal epithelial cells *in vivo* and MDCK cells. Cell types along the renal tubule differ in the expressed complement of SNAREs as well as in their subcellular localization. Altogether, our results suggest that the modulation of SNARE expression and localization is used by epithelial cells as a mechanism to achieve the known plasticity of sorting phenotypes.

MATERIALS AND METHODS

Antibodies. Rabbit polyclonal antibodies against rat syntaxins 2, 3, and 4 were generated against bacterially expressed glutathione-S-transferase (GST) fusion proteins of the cytoplasmic domains of the respective syntaxin isoforms as described previously (32). In addition, polyclonal antibodies against the ~100 NH₂-terminal amino acids of human syntaxins 3 and 4 were raised. All antibodies were affinity purified using the respective syntaxin cytoplasmic domains that were separated from GST by thrombin cleavage and coupled to Affigel (Bio-Rad, Richmond, CA). Rabbit antiserum was raised against a GST fusion protein of the cytoplasmic domain of rat endobrevin. The expression plasmid was a gift from Wanjin Hong (Institute for Molecular and Cell Biology, Singapore). The endobrevin antibody was affinity purified as described above. As confirmatory controls, the following antibodies were used: affinity-purified polyclonal rabbit antibodies against rat syntaxins 2, 3, and 4 (described in Ref. 30; kindly provided by Mark Bennett and Beatriz

Quiñones, University of California Berkeley); a monoclonal antibody against human syntaxin 4 (Transduction Laboratories); and a polyclonal antibody against the cytoplasmic domain of rat syntaxin 2 (Synaptic Systems, Göttingen, Germany). Rabbit antibodies against the 33- and 70-kDa subunits of the vacuolar H⁺-ATPase (51) were kindly provided by Xiao-Song Xie (University of Texas, Southwestern Medical Center). Mouse monoclonal anti-band 3 antibody was kindly provided by Michael Jennings (University of Arkansas for Medical Sciences). Rabbit polyclonal anti-aquaporin-1 was obtained from Chemicon (Temecula, CA). Mouse monoclonal anti-calbindin D28 was from Sigma (St. Louis, MO). Rhodamine-labeled lectin *Dolichos biflorus* agglutinin was from Vector Labs (Burlingame, CA). Sheep polyclonal anti-Tamm-Horsfall glycoprotein was purchased from Biogenesis (Brentwood, NH).

Immunoblot analysis. Male Sprague-Dawley rats were euthanized by decapitation, and the kidneys were removed. Cortex and medulla were microdissected under a microscope and finely minced with a razor blade. Tissue was homogenized in ice-cold PBS with protease inhibitors (phenylmethylsulfonyl fluoride, leupeptin, pepstatin, chymostatin, antipain, benzamide, trasyolol) using a Dounce homogenizer. The homogenates were first spun at 500 g for 2 min to pellet nuclei. The supernatants were then centrifuged at 13,000 g for 20 min to obtain the membrane fractions. Membrane fractions and supernatants (equal protein amounts) were separated by 15% SDS-PAGE. The proteins were transferred to polyvinylidene difluoride membranes and analyzed using the affinity-purified polyclonal anti-syntaxins 2, 3, or 4 antibodies, horseradish peroxidase-conjugated secondary antibodies (Jackson ImmunoResearch, West Grove, PA), and ECL (Pierce, Rockford, IL).

Immunolocalization in tissue sections. Sprague-Dawley male rats (230–250 g) were anesthetized by intraperitoneal administration of pentobarbital sodium, systemically heparinized, and perfused via the left ventricle with 4% paraformaldehyde in PBS with 1 mM calcium and 1 mM magnesium for 20 min. The kidneys were removed and cut into small blocks, which were further fixed in the same fixative overnight at 4°C. The blocks were dehydrated through serial ethanol and xylene and embedded in paraffin. Immunostaining was carried out on 5- μ m sections. After deparaffinization and rehydration to PBS, the sections were pressure-cooked in 10 mM citric acid buffer, pH 6.0, for antigen retrieval. The sections were blocked with 3% BSA, 2% Triton X-100 in PBS and incubated with the indicated antibodies overnight at 4°C. To identify different tubule segments and cell types, double immunofluorescence staining of the same or serial sections was performed with the following: mouse anti-calbindin for the principal cells of connecting tubules and collecting ducts in the cortex (42); anti-H⁺-ATPase polyclonal antibodies and anti-band 3 monoclonal antibody for intercalated cells (2); rabbit anti-aquaporin-1 polyclonal antibody for proximal tubule and descending limb of the loop of Henle (45); sheep anti-Tamm-Horsfall glycoprotein for thick ascending limb of the loop Henle (65); and rhodamine-labeled *D. biflorus* agglutinin for proximal tubules and collecting ducts (65). The reactions were visualized by fluorescein- or Texas red-labeled secondary antibodies (Jackson ImmunoResearch). Signals for syntaxins 3 and 4 were amplified by incubating with Alexa 488-labeled rabbit anti-FITC antibody (Molecular Probes, Eugene, OR) subsequent to the FITC-labeled secondary antibodies. Syntaxin 2 signals were amplified by tyramide signal amplification (TSA-Direct, NEN Life Science Products, Boston, MA). For simultaneously localizing two proteins recognized by rabbit primary antibodies, FITC-

or rhodamine-labeled Fab fragments of the secondary antibody (Jackson ImmunoResearch) were used after incubation with the first rabbit primary antibody. The sections were shortly fixed with 4% paraformaldehyde, then incubated with the second rabbit primary antibody, followed by Texas red- or FITC-labeled secondary antibody.

To eliminate cross-reactivity of syntaxin antibodies against related syntaxins, primary antibodies were preincubated with 2% native and 2% heat/SDS-denatured total lysates of *Escherichia coli*-expressing GST fusion proteins of the non-relevant syntaxins. For example, bacterial lysates of syntaxins 2 and 3 were added to anti-syntaxin 4 antibody incubations. The fluorescent staining was analyzed using a confocal laser scanning microscope (TCS-NT, Leica, Bensheim, Germany).

Expression levels of syntaxins and endobrevin in different tubule segments were estimated as follows. Fluorescent images of multiple fields were acquired using identical exposure settings, ensuring that the regions of brightest signals did not exceed the maximal intensity of the eight-bit signal. The background was subtracted using Adobe Photoshop. Pixel values of each tubule type were integrated using National Institutes of Health IMAGE 1.61 software. For each type of tubule, at least three tubules were counted. The intensity values were divided by the number of cells in each tubule and averaged.

Cell culture, transfection, and immunolocalization in cultured cells. MDCK strain II cells were cultured in MEM containing Earle's salts and supplemented with 10% FBS, 100 U/ml penicillin, and 100 μ g/ml streptomycin in 5% CO₂. Cells were cultured on Transwell polycarbonate filters (12 mm, 0.4- μ m pore size, Corning Costar, Cambridge, MA) for 4–5 days (polarized) or for 1 day (semipolarized). For expression of COOH-terminal epitope-tagged syntaxin 4, human syntaxin 4 cDNA was cloned into a modified pcDNA4/TO vector (Invitrogen) to add two COOH-terminal myc epitope tags in tandem and one hexahistidine tag to the COOH terminus. MDCK cells were transfected, and stable clones were isolated by Zeocin selection. The additional epitope tags did not interfere with the correct polarized targeting of syntaxin 4 and allowed detection at the plasma membrane by surface immunolabeling.

For surface staining of epitope-tagged syntaxin 4, cells on Transwell filters were incubated with anti-myc antibody (9E10) antibody for 2 h on ice. After several washes, cells were fixed with 4% paraformaldehyde in PBS and incubated with FITC-labeled secondary antibody. The culture and im-

muno-staining of MDCK cells in collagen gels have been described previously (52).

RESULTS

Only membrane-bound isoforms of syntaxins 2, 3, and 4 are expressed in rat kidney. Polyclonal antibodies were raised against GST fusion proteins of the full-length cytoplasmic domains of rat syntaxins 2, 3, and 4. The antibodies were affinity purified using the immobilized, thrombin-cleaved syntaxin domains and tested for their isoform specificity by Western blot analysis. A low degree of cross-reactivity was observed, which could be completely eliminated by preincubating each syntaxin antibody with the GST fusion proteins of the others, resulting in specific signals. Therefore, preincubation was used for all subsequent experiments.

Isoforms of syntaxins 2 and 3, derived from alternative RNA splicing, have been identified previously (20, 22, 53, 55). They all differ only in the COOH-terminal parts of the molecules, and our antibodies are predicted to react with all of them. Some of these isoforms lack COOH-terminal transmembrane anchors, and previous results indicated that some of the syntaxin 2 isoforms are not membrane bound and purify in soluble cytoplasmic fractions (53). To investigate whether soluble syntaxin isoforms may be expressed in rat kidney, medulla and cortex were dissected, and total membrane and cytosol fractions were analyzed by immunoblotting. Figure 1 shows that all syntaxins are detected exclusively in the membrane fractions. Only single bands of the expected size of the full-length proteins are detected, except for syntaxin 2, which shows a faint additional band of slightly higher molecular weight. No significant differences were detected between renal cortex and medulla. These results indicate that the majority of syntaxins 2, 3, and 4 in rat kidney are membrane-associated isoforms.

The apical and basolateral localization of syntaxins 3 and 4 are conserved in all renal epithelial cell types. In MDCK cells, syntaxins 3 and 4 are mutually exclusively localized at the apical and basolateral plasma membrane domains, respectively, where they function

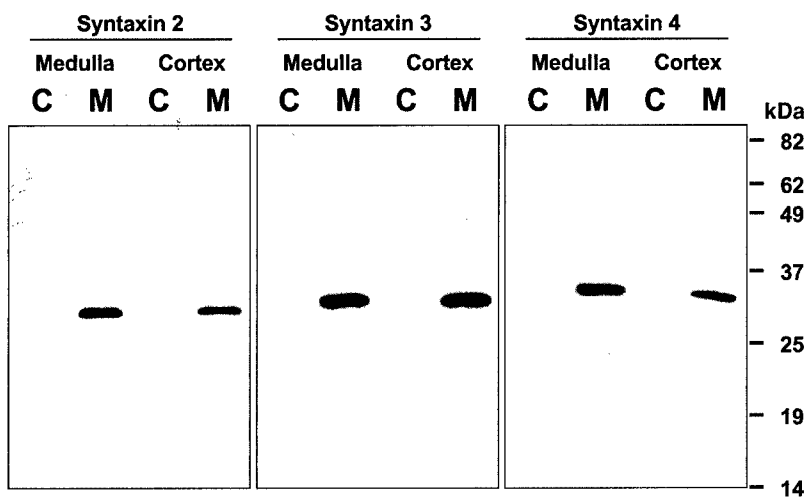


Fig. 1. Western blot analysis of syntaxins 2, 3, and 4 in rat kidney. Cortex and medulla were dissected under a microscope. Cytosolic (C) and membrane (M) protein fractions were isolated (see MATERIALS AND METHODS). Using affinity-purified antibodies against syntaxins 2, 3, and 4, 5 μ g for syntaxins 2 and 3 or 20 μ g for syntaxin 4 of total protein/lane were investigated by immunoblotting. Note that all syntaxins fractionate with total membranes and that their abundance is similar between renal cortex and medulla.

in polarized pathways (30, 31). To determine whether this is a general feature of all epithelial cell types along the renal tubule, we investigated their expression and localization by confocal immunofluorescence microscopy on rat kidney tissue sections. Individual tubule segments and cell types were identified by colabeling with lectins or antibodies against well-characterized marker proteins (see MATERIALS AND METHODS). Figure 2

shows that without exception, syntaxins 3 and 4 are restricted to the apical and basolateral plasma membrane domains, respectively, in all renal epithelial cell types.

The expression level of syntaxin 3 varies significantly between different cell types (for semiquantitative analysis, see Fig. 7). It is most highly expressed in proximal convoluted tubules, in which it localizes to

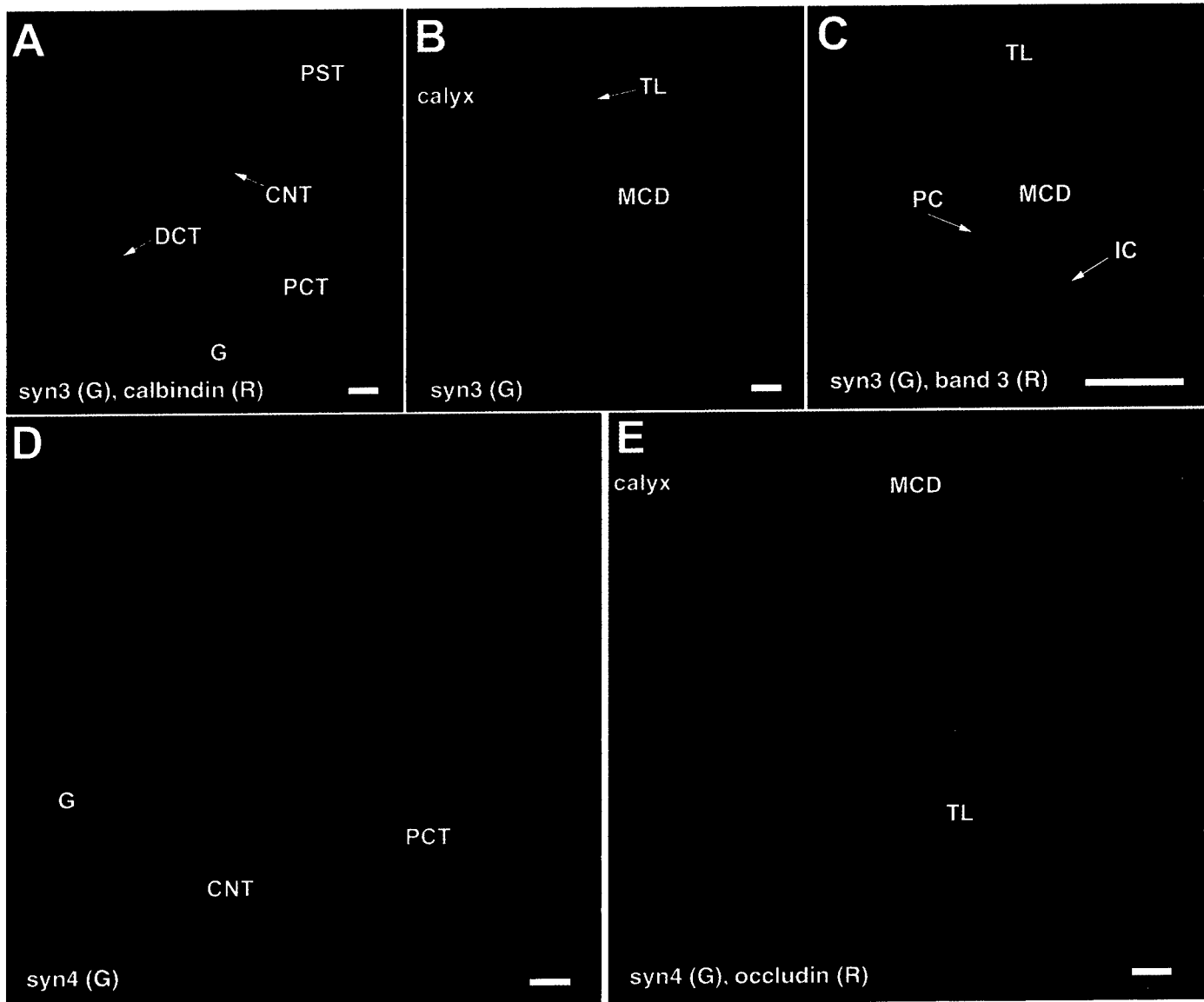


Fig. 2. Localization of syntaxins 3 and 4. Rat kidney sections were immunostained using affinity-purified syntaxin antibodies and colabeled with various segment-specific markers. Representative examples are shown. *A*, *B*, and *C*: syntaxin 3 labels in green (G). *D* and *E*: syntaxin 4 labels in green. Colabeling in red (R) is for calbindin (*A*), band 3 (*C*), and occludin (*E*). *A* and *D* show representative fields of renal cortex, whereas *B*, *C*, and *E* show medullary fields. Note that the subcellular localizations of syntaxins 3 and 4 are always restricted to the apical or basolateral plasma membrane, respectively. The intensity of staining is variable for syntaxin 3, with the highest level in the convoluted part of proximal tubules. Syntaxin 3 expression is weakest in the thick ascending limb of the loop of Henle. Syntaxin 4 is more uniformly expressed with the highest level in proximal tubules (*D*). Note that syntaxin 4 localizes to both the lateral and the basal membranes of all epithelial cell types. Abbreviations for this and subsequent figures are syn3 and syn4, Syntaxins 3 and 4, respectively; ATL, ascending thin limb of the loop of Henle; CCD, cortical collecting duct; CNT, cortical connecting tubule; DCT, distal convoluted tubule; DTL, descending thin limb of the loop of Henle; G, glomerulus; IC, intercalated cell; MCD, medullary collecting duct; PC, principal cell; PCT, proximal convoluted tubule; PST, proximal straight tubule; TAL, thick ascending limb of the loop of Henle; TL, thin limb of Henle. Bars, 20 μ m.

the apical brush border (Fig. 2A). The expression level per cell is at least 10-fold lower in the thick ascending loop of Henle. Expression levels in other tubule segments are intermediate (Fig. 2, B and C).

In contrast to syntaxin 3, the expression level of syntaxin 4 is more uniform along the renal tubule. It is evenly distributed along the basal and lateral plasma membrane domains of all cell types. Syntaxin 4 also prominently localizes to the basal infoldings in cell types that possess them, such as proximal tubule cells (Fig. 2D).

All immunostaining results were confirmed using independently raised antibodies against rat syntaxins 3 and 4 (see MATERIALS AND METHODS). Furthermore, poly- and monoclonal antibodies against human syntaxins 3 and 4 were used in human kidney. In all cases, identical results were obtained (data not shown). Together, these results indicate that the mutually exclusive localizations of syntaxins 3 and 4 are highly conserved, suggesting that their apical- and basolateral-specific functions, respectively, are critical for the maintenance of epithelial cell polarity. The finding that the expression level of syntaxin 3 is highly cell type dependent indicates that syntaxin 3-dependent apical trafficking pathways vary among cell types and that renal epithelial cells have the ability to regulate its expression level, depending on their trafficking phenotype.

The polarity of syntaxin 2 is reversed between renal epithelial cell types. Investigation of syntaxin 2 localization revealed an unexpected pattern (Fig. 3). Expression is highest in medullary collecting ducts and the loop of Henle, where syntaxin 2 is restricted to the apical domain (Fig. 3, B and C). In contrast, most cortical tubule segments do not express detectable levels of syntaxin 2, except for the principal cells of connecting tubules and collecting ducts (Fig. 3A). In these

cells, syntaxin 2 is localized to the basolateral domain. Therefore, the localization of syntaxin 2 is inverted between cortical and medullary principal cells. This suggests that localizing syntaxin 2 to different plasma membrane domains may be part of a mechanism to modulate epithelial sorting phenotypes. Again, the results could be confirmed with two independently raised anti-syntaxin 2 antibodies, resulting in identical staining patterns in rat and mouse kidney (not shown).

Syntaxins in intercalated cells. A striking example of the plasticity of epithelial sorting phenotypes are intercalated cells of the cortical connecting tubules and collecting ducts. One of their main functions is the maintenance of acid-base homeostasis. They exist in two varieties: α -cells, which secrete protons and target the H^+ -ATPase apically, and β -cells, which secrete bicarbonate and target the H^+ -ATPase basolaterally (1, 9). In addition, a bicarbonate exchanger and other proteins are differentially targeted in these two cell types. It has been suggested that α -cells can convert into β -cells and vice versa, depending on the acid-base status of the organism (8). Therefore, it is thought that the conversion between α - and β -cells involves an inversion of cell polarity, which implies that the molecular machineries for vesicle targeting would be inverted. If this were the case, we would expect that one or more plasma membrane syntaxins would be differently localized between α - and β -cells. To test this theory, cortical α - and β -cells were identified by immunostaining with an antibody against the 70-kDa subunit of H^+ -ATPase. The localizations of syntaxins 2, 3, and 4 were defined by colabeling. Figure 4 shows that the apical and basolateral localization, respectively, of syntaxins 3 (Fig. 4B) and 4 (Fig. 4C) do not change between α - and β -intercalated cells. Syntaxin 2 is expressed and basolaterally localized in the neighboring principal cells as described above but is undetectable in

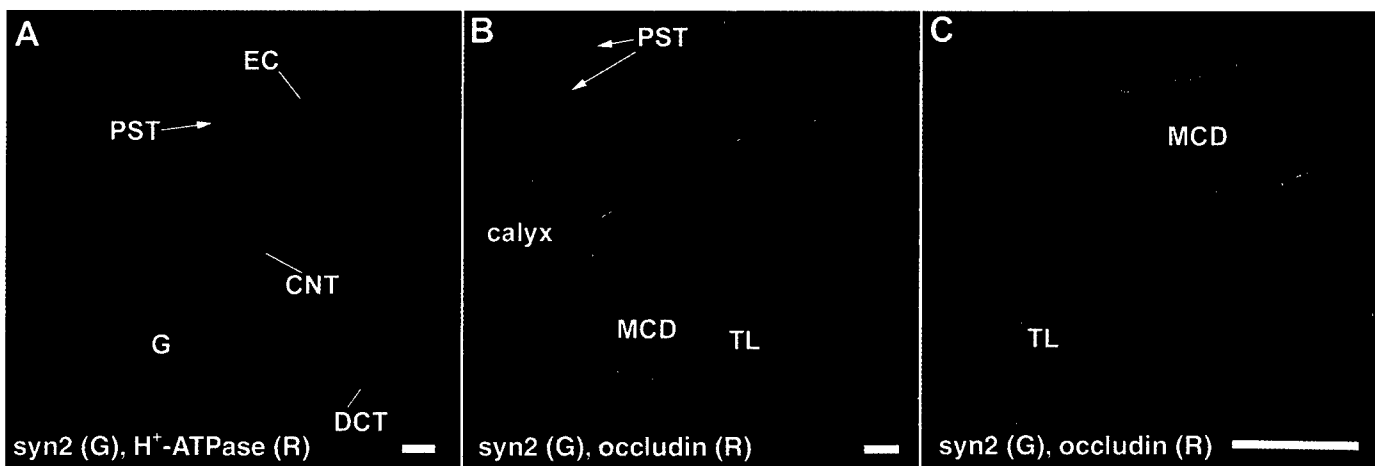


Fig. 3. Localization of syntaxin 2. Rat kidney sections were immunostained for syntaxin 2 (syn2; A–C, green) and vacuolar H^+ -ATPase (A, red), or the tight junction protein occludin (B and C, red). A: representative field of kidney cortex. B: cortex (top left) and medulla (bottom right). C: higher magnification of medullary tubules. Syntaxin 2 is expressed in endothelial cells (EC) of the glomeruli (G) and between the tubules. Of the cortical epithelial cells, syntaxin 2 is only expressed in the principal cells of the connecting tubules and collecting ducts (A), in which it is basolaterally localized. In contrast, in the medulla, syntaxin 2 is apically localized in the thin limb of the loop of Henle and principal cells of collecting ducts (B and C). Bars, 20 μ m.

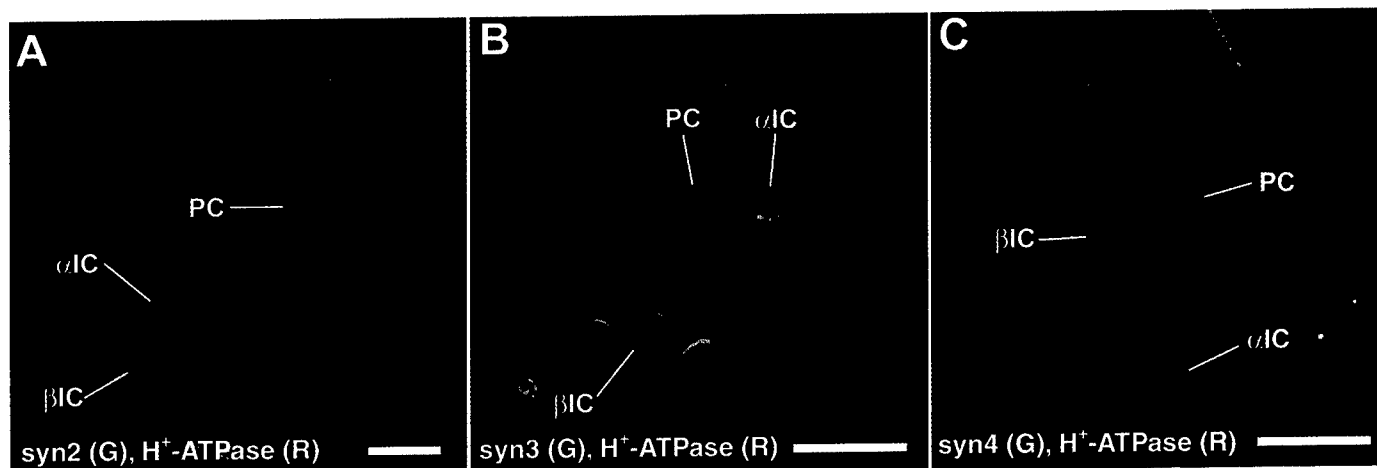


Fig. 4. Syntaxin localization in α (α IC)- and β -IC (β IC). Cortical α IC and β IC were identified by immunolocalization of the vacuolar H^+ -ATPase (red), which is apical in α IC and basolateral in β IC. PC are negative for the H^+ -ATPase. Syntaxin 2 (A) is only expressed in PC but not in intercalated cells. Syntaxin 3 (B) is expressed and apically localized in all 3 cell types. Similarly, syntaxin 4 (C) is basolaterally localized in all 3 cell types. Bars, 20 μ m.

intercalated cells (Fig. 4A). The differential sorting phenotypes of α - and β -intercalated cells can therefore not be explained by differential localization of these plasma membrane syntaxins. These results make it unlikely that polarized membrane trafficking in general is inverted between these cell types.

Endobrevin is highly expressed in apical endosomes in proximal tubules and intercalated cells. Endobrevin/vesicle-associated membrane protein-8 is a member of the syntaxobrevin family of v-SNAREs and implicated in early and/or late endosome fusion in nonpolarized cells (3). In polarized MDCK cells, green fluorescent protein (GFP)-tagged endobrevin has been reported to cycle between endosomes and the apical plasma membrane, indicating that it may be involved in an apical endocytic/recycling pathway in epithelial cells (58). We found that proximal tubule cells exhibit the highest expression levels of endobrevin. In these cells, endobrevin localizes to a narrow band of vesicles clustered underneath the apical brush border (Fig. 5A). Costaining for endobrevin and syntaxin 3 reveals no overlap (Fig. 5B). This is the characteristic localization of the extensive endocytic apparatus of proximal tubules involved in reabsorption of proteins from the ultrafiltrate (9, 37). The prominent localization of endobrevin on these apical endosomes, together with the previous finding of cycling of GST fusion protein-endobrevin through the apical plasma membrane of MDCK cells suggests that this protein may function as a v-SNARE on vesicles that recycle back to the apical brush border of proximal tubule cells.

Endobrevin is also highly expressed in intercalated cells of the connecting tubules and collecting ducts (Fig. 5, C and D). In α -intercalated cells, endobrevin colocalizes with the vacuolar H^+ -ATPase in the apical cytoplasm. In contrast, in β -intercalated cells endobrevin is distributed throughout the cytoplasm and shows no colocalization with the H^+ -ATPase. The vacuolar H^+ -ATPase is known to cycle between endosomes and

either apical or basolateral plasma membrane in α - and β -intercalated cells, respectively (1, 9). This result therefore suggests that endobrevin is involved in the apical recycling pathway of the H^+ -ATPase in α -intercalated cells, whereas a different v-SNARE is likely involved in basolateral recycling in β -intercalated cells. Lower amounts of endobrevin are expressed in all other tubule epithelial cells in intracellular vesicles (see Fig. 7).

The in vivo localization of syntaxin 4 differs from that in cultured MDCK cells. The subcellular localization of syntaxin 4 in vivo, as described above, differs from its localization in cultured MDCK cells. Endogenous syntaxin 4 is concentrated at the lateral plasma membrane domain in polarized MDCK cells cultured on Transwell filters (Fig. 6A). In contrast, very little if any syntaxin 4 is detectable at the basal domain. This result could be confirmed in stably transfected MDCK cells expressing COOH-terminal myc-tagged syntaxin 4. The epitope tags are designed to protrude out of the cells, allowing surface labeling of live, intact cells. The subcellular localization of myc-tagged syntaxin 4 is identical to the endogenous protein (Fig. 6B).

In contrast, in subconfluent, semipolarized MDCK cells, syntaxin 4 localizes to the basal membrane that is in contact with the substratum (Fig. 6C). Therefore, during the development of a polarized monolayer, syntaxin 4 relocates from the basal to the lateral domain. The absence of a basal syntaxin 4 signal in polarized MDCK cells is not an artifact of the acquisition of confocal optical sections in the X-Z direction because the basal signal is clearly detectable in subconfluent cells under the same conditions. This result predicts that the majority of basolateral vesicle traffic in MDCK cells will be toward the lateral, not the basal, plasma membrane domain. This is in excellent agreement with our recent experiments in which basolateral trafficking of post-Golgi transport vesicles in MDCK cells was monitored by time-lapse fluorescence microscopy (Kre-

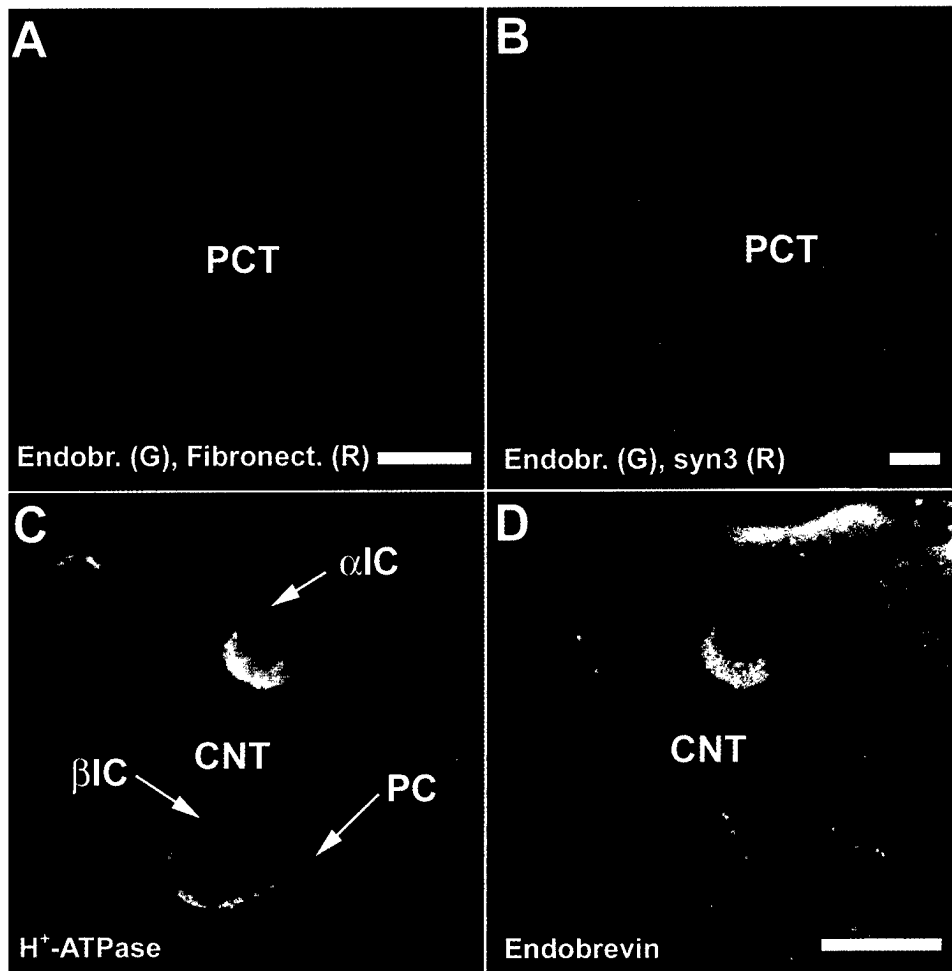


Fig. 5. Localization of endobrevin. Endobrevin is expressed in all epithelial cell types of the renal tubule, where it localizes to intracellular vesicles. It is most highly expressed in the convoluted proximal tubule [endobrevin (Endobr) is green, fibronectin is red, and nuclei are blue; A], in which it localizes to the prominent endosomes underneath the apical brush border. C and D: cortical collecting tubule costained for the vacuolar H^+ -ATPase and endobrevin, respectively. In α IC, endobrevin is highly expressed and colocalizes with the H^+ -ATPase in the apical region of the cells. In contrast, the expression level of endobrevin is lower in β IC and distributed throughout the cytoplasm. Expression is lowest in the PC. Bars, 10 μ m.

itzer G, Schmoranz J, Low SH, Li X, Gan Y, Weimbs T, Simon SM, and Rodriguez-Boulan E, unpublished observations). All "basolateral" fusion events occurred at the lateral domain, whereas no fusion was detected at the basal domain. In contrast, basolateral fusion can fuse efficiently with the basal membrane of nonpolarized MDCK cells. Together, these results suggest that the subcellular localization of syntaxin 4 can serve as an indicator of the location of fusion sites in the trafficking pathways that depend on this SNARE.

In contrast to polarized MDCK cells, collecting duct cells in vivo, those from which MDCK cells are derived, exhibit very prominent basal staining of syntaxin 4 in addition to the lateral signal (Fig. 2). The same is the case for all other renal epithelial cell types in vivo. This suggests that the entire basolateral plasma membrane of renal epithelial cells in vivo is fusion competent for basolateral trafficking. Therefore, these results indicate that MDCK cells cultured on Transwell filters do not correctly reproduce the in vivo phenotype with respect to the localization of syntaxin 4 and basolateral trafficking. We investigated whether a culture system that more closely approximates the renal tubule may yield different results. MDCK cells can be cultured in gels of type I collagen, in which they form hollow spherical cysts that are lined by a monolayer of polar-

ized cells. Under these conditions, syntaxin 4 localized all along the basal and lateral plasma membrane domains identically to native collecting duct cells in vivo. This suggests that MDCK cell culture in three-dimensional cysts more closely approximates the in vivo situation than does two-dimensional culture on Transwell filters and that vesicle fusion may occur all along the basolateral membrane.

DISCUSSION

Here, we report differences and similarities in the in vivo localization of plasma membrane syntaxins in the renal epithelium compared with the most widely studied in vitro epithelial model system, the MDCK cell line. One important finding is that the mutually exclusive localizations of syntaxins 3 and 4 are strictly conserved in all epithelial cell types. Without exception, syntaxin 3 localizes to the apical and syntaxin 4 to the basolateral domain. Syntaxin 3 has also previously been found to be apical specific in the Caco-2 colon epithelial cell line (6, 12, 17, 54) and in hepatocytes (15). Syntaxin 4 has been found on the basolateral plasma membrane of pancreatic acinar cells (16). Collectively, these results indicate that the polarized apical or basolateral localization, respectively, of syntaxins 3 and 4 is a common feature of

epithelial cells. This suggests that the strict separation of these two syntaxins is necessary for the establishment of distinct sites of polarized vesicle exocytosis and hence for the development and integrity of cell polarity.

We were unable to confirm previous results by another group that reported opposite polarities of syntaxins 3 and 4 in rat kidney (5, 35, 36). However, our results are in agreement with data by Lehtonen et al. (28), who used an independently raised antibody to investigate the localization of syntaxin 3 in developing mouse kidney and observed identical expression and subcellular localization, as presented here. We could

confirm our immunolocalization data with several independent antibodies against syntaxins 3 and 4 in rat, mouse, and human kidney sections. In all cases, identical results were obtained. The cause for the aforementioned contradictory results remains unknown.

It is plausible that the cellular expression level of a given SNARE is at least a rough measure of the amount of traffic that depends on this SNARE and occurs in a given cell. For example, neurons express very high quantities of syntaxin 1, SNAP-25, and synaptobrevin, which are involved in synaptic vesicle exocytosis. Even a modest decrease in protein expression of syntaxin 1 and SNAP-25 results in decreased insulin secretion from pancreatic β -cells from islets in a rodent model of type 2 diabetes (43). Similarly, a 50% reduction in the expression level of syntaxin 4 in a heterozygous knockout mouse causes inhibition of GLUT4 transport to the plasma membrane in skeletal muscle cells (63). This suggests that the expression levels of SNAREs must be tightly regulated in concert with the cellular requirements for trafficking pathways that involve a given SNARE. Our results show that the expression level of syntaxin 4 is relatively uniform in all renal epithelial cell types (Fig. 7). This suggests that it performs a function that is required by all cell types. In nonepithelial cells, syntaxin 4 has been implicated in granule exocytosis in mast cells (50) and platelets (13) and insulin-stimulated GLUT4 translocation in skeletal muscle (63) and adipocytes (34, 40, 49, 60). In MDCK cells, syntaxin 4 is required for basolateral delivery of newly synthesized vesicular stomatitis virus G protein (26). This variety of trafficking pathways together with the uniform expression in renal epithelial cells suggest that syntaxin 4 functions as a "housekeeping" plasma membrane t-SNARE in many or all mammalian cells and that the "housekeeping trafficking pathways" in nonepithelial cell types correspond to pathways that lead to the basolateral domain of epithelial cells. Conceptually, the basolateral surfaces of virtually all epithelial cells face a similar environment, i.e., the underlying basement membrane and endothelial or connective tissue cells. It is there-

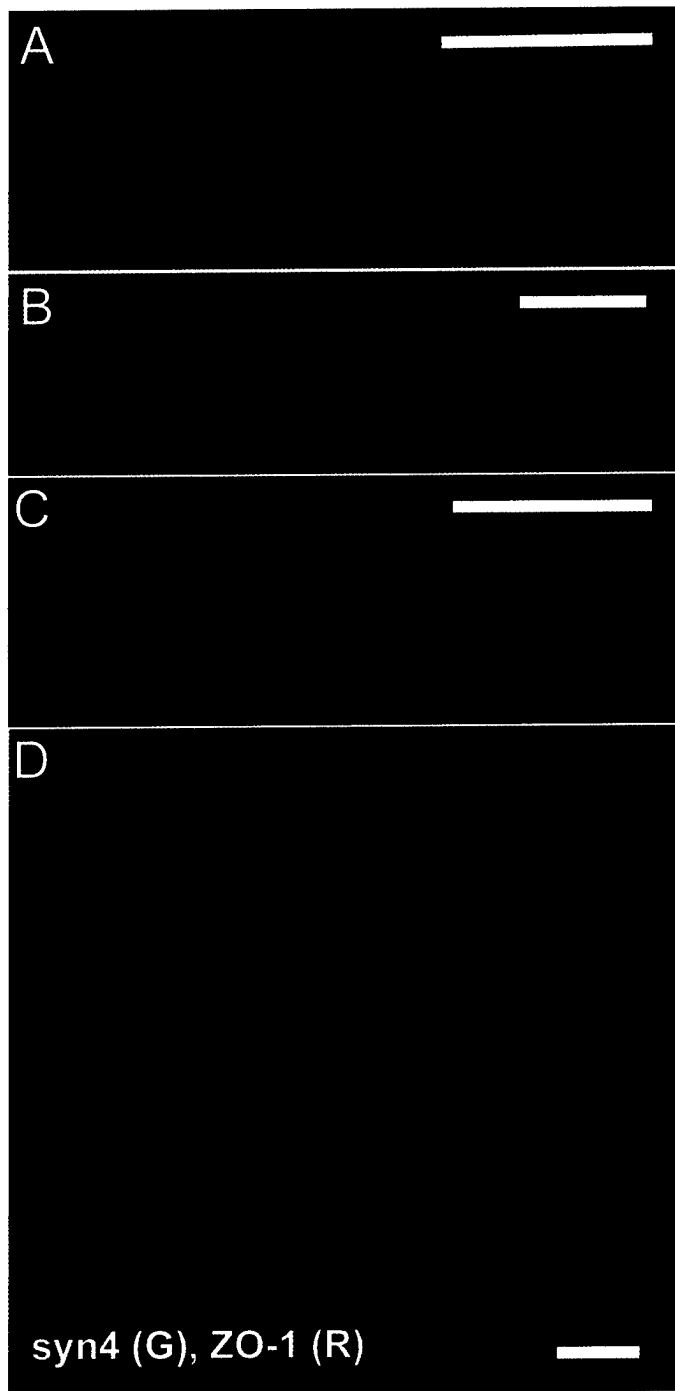


Fig. 6. Localization of syntaxin 4 in Madin-Darby canine kidney (MDCK) cell changes, depending on the degree of cell polarity and the culture system. *A*: MDCK cells were cultured on Transwell filters for 5 days and colabeled for endogenous syntaxin 4 (green) and the tight junction marker zonula occludens-1 (ZO-1; red). Shown is a confocal X-Z optical section with the apical plasma membrane at the top. Note the exclusively lateral localization of syntaxin 4. *B*: MDCK cells stably expressing COOH-terminal myc-tagged syntaxin 4 were cultured as above and subjected to surface labeling using anti-myc antibody. Note that the localization of recombinant syntaxin 4 is identical to that of the endogenous protein. *C*: the same cells as in *B* were cultured for 1 day to yield semipolarized cells. Surface immunolabeling revealed that under these conditions syntaxin 4 localizes to both the lateral and basal plasma membrane domains. *D*: MDCK cells were cultured in type-I collagen for the development of 3-dimensional cysts. Endogenous syntaxin 4 (green) and ZO-1 (red) were stained by coimmunolabeling and imaged by confocal fluorescence microscopy. Note that under these conditions syntaxin 4 localizes to both the basal and the lateral plasma membrane domains, resembling its localization in renal epithelial cells in vivo. Bars, 20 μ m.

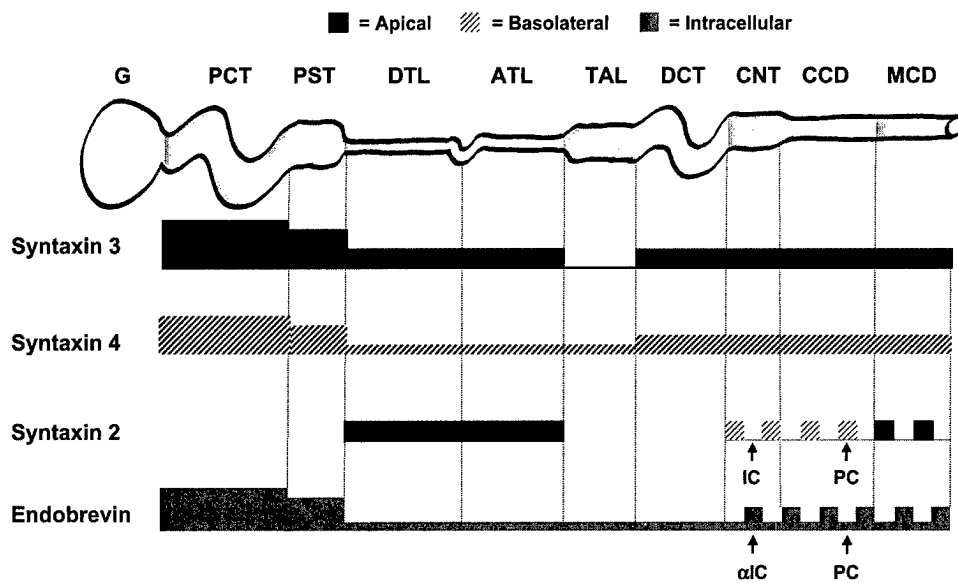


Fig. 7. Summary of expression and subcellular localization of syntaxins 2, 3, and 4 and endobrevin in different segments of the renal tubule. Shown is a schematic representation of the renal tubule with the segments indicated. The expression levels per cell of the SNAREs were estimated by integrating the pixel values of each tubule type as described in MATERIALS AND METHODS. The heights of the bars represent the relative expression levels for each SNARE. For abbreviations, see legend to Fig. 2.

fore likely that most epithelial cell types have similarly abundant common basolateral trafficking pathways that depend on syntaxin 4. Plausible examples are the secretion of extracellular matrix proteins, the recycling of membranes after endocytosis of growth factor receptors, etc.

In contrast, trafficking toward the apical surface of epithelial cells is expected to be highly cell type dependent because the environment that an epithelial cell faces apically can differ dramatically. This agrees well with our finding that the expression level of syntaxin 3 varies significantly among the renal tubule cell types. We have previously shown that syntaxin 3 is involved in two pathways in MDCK cells: apical delivery of newly synthesized membrane proteins and the apical recycling of apically internalized membranes (31). In a typical mammalian cell, the volume of recycling far outweighs that of biosynthetic traffic to the plasma membrane (57, 59). This difference is expected to be even more pronounced in nonproliferative, nonsecretory cell types such as renal tubule cells. Therefore, a high expression level of syntaxin 3 would be mostly indicative of a highly active apical recycling pathway. Indeed, we find the highest level of syntaxin 3 expression in the convoluted proximal tubule. This cell type exhibits a very high apical endocytosis rate for the absorption of proteins from the ultrafiltrate (11, 29, 47) and consequently recycles large amounts of membrane back to the apical plasma membrane. Interestingly, the highest expression level of the v-SNARE endobrevin is also found in the convoluted proximal tubule, and it localizes on apical endosomes underneath the brush border. GFP-tagged endobrevin has been reported to cycle through the apical plasma membrane of MDCK cells (58). We therefore suggest that in renal epithelial cells endobrevin functions as the v-SNARE on recycling vesicles that fuse with the apical plasma membrane utilizing syntaxin 3.

Whereas the polarities of syntaxins 3 and 4 are conserved throughout the renal tubule, the polarity of

syntaxin 2 changes, depending on the cell type. Syntaxin 2 localizes to the basolateral plasma membrane in cortical principal cells, while it is apical in the principal cells of the medulla and in the thin loop of Henle. No expression is detectable in the other cell types. This suggests that syntaxin 2 is involved in a specialized trafficking pathway and that this pathway differs between cortical and medullary principal cells. We are unaware of a trafficking pathway whose polarity is known to be reversed in these two cell types. However, differences between medullary and cortical collecting duct principal cells have been reported previously. The apical renal urea transporter is expressed in medullary principal cells but absent in cortical principal cells (46). Also, medullary, but not cortical, principal cells exhibit prominent cytoplasmic fodrin staining (14). To date, syntaxin 2 has been implicated in two fusion events: zymogen granule exocytosis in pancreatic acinar cells (19) and the fusion of the acrosome with the plasma membrane of spermatozoa (25). Because these cell types differ significantly from renal epithelial cells, it is impossible to predict in which pathways syntaxin 2 may be involved, and functional studies will be required.

α - and β -Intercalated cells are classic examples of inverted sorting phenotypes between different epithelial cell types. They differ in their targeting of the vacuolar H^+ -ATPase and other proteins (1, 9), which has led to the idea that cell polarity may be generally inverted between α - and β -intercalated cells. However, our finding that both cell types exhibit identical polarities of syntaxins 3 and 4 makes this very unlikely. Syntaxin 2 is not expressed in intercalated cells and can therefore play no role in differential H^+ -ATPase targeting. It is possible that other, unidentified syntaxins may be differentially expressed at the plasma membranes of intercalated cells, but these would likely serve a very specialized trafficking pathway. We consider it more likely that the H^+ -ATPase is differentially sorted into "conventional" apical or basolateral

trafficking pathways in α - and β -intercalated cells, respectively, which utilize syntaxin 3 or 4. This would predict that different classes of Golgi- or endosome-derived transport vesicles would be utilized for H^+ -ATPase trafficking in α - and β -intercalated cells, which would likely contain different v-SNAREs. Interestingly, we found that endobrevin is highly expressed in intercalated cells and colocalizes with the H^+ -ATPase in α - but not β -intercalated cells. This suggests that endobrevin is involved in apical H^+ -ATPase trafficking in α -intercalated cells, whereas another v-SNARE would perform the equivalent function in β -intercalated cells.

Cultured MDCK cells are widely used as a model system for studying membrane trafficking. Recent attention has focused on the question of whether exocytic events occur all along the apical or basolateral plasma membrane domains or whether there are localized regions of vesicle fusion. It has been proposed that fusion events occur at the region of the tight junctions. This is based on the finding that several proteins implicated in membrane fusion localize there. These include rab8 (21), rab3b (61), rab13 (64), the sec6/8 complex or exocyst (18), and VAP-A (27). It had seemed odd that syntaxins apparently did not specifically localize to the tight junctions in MDCK cells. Recently, for the first time, the sites of fusion of post-Golgi transport vesicles in polarized MDCK cells could be identified by time-lapse fluorescence microscopy using GFP-tagged apical and basolateral marker proteins (Kreitzer G, Schmoranzler J, Low SH, Li X, Gan Y, Weimbs T, Simon SM, and Rodriguez-Boulant E, unpublished observations). These experiments demonstrated that basolateral transport vesicles fuse all along the lateral membrane, not just at the tight junctions. However, no fusion events were observed at the basal membrane. These findings agree well with the localization of syntaxin 4 in these cells, which is present along the lateral, but not basal, membrane. In contrast, syntaxin 4 does localize to the basal membrane of subconfluent, not fully polarized, MDCK cells, which agrees well with the observation of basal fusion events under these conditions (Kreitzer G, Schmoranzler J, Low SH, Li X, Gan Y, Weimbs T, Simon SM, and Rodriguez-Boulant E, unpublished observations). Altogether, these results suggest that the subcellular localization of syntaxins identifies the corresponding fusion sites. Because we find that syntaxin 4 localizes to both the lateral and basal domains of renal epithelial cells in vivo, this in turn suggests that vesicle fusion occurs all along the basolateral plasma membrane in vivo. Therefore, MDCK cells cultured on Transwell filters (the usual culture method) do not appear to faithfully reproduce the in vivo phenotype with respect to basolateral vesicle fusion. MDCK cells cultured as three-dimensional cysts in type-I collagen, however, target syntaxin 4 correctly to both domains.

In conclusion, we have shown that the expression levels of SNAREs and their subcellular localizations can differ very significantly among the epithelial cell types along the renal tubule. This agrees well with the

known differences in epithelial trafficking phenotypes and suggests that regulation of SNARE expression and localization serves as a cellular mechanism to achieve, at least in part, these distinct phenotypes. In turn, the dysregulation of SNARE expression or localization may lead to abnormal intracellular trafficking and disease. Well-known examples of diseases involving epithelial cells and defects in polarized trafficking include polycystic kidney disease and microvillus inclusion disease (48).

We appreciate the gifts of reagents by Drs. Mark Bennett and Beatriz Quiñones (University of California Berkeley), Wanjin Hong (Institute for Molecular and Cell Biology, Singapore), Michael Jennings (University of Arkansas for Medical Sciences) and Xiao-Song Xie (University of Texas, Southwestern Medical Center). Elizabeth Loh and Zhizhou Zhang contributed to the construction of the expression vector for epitope-tagged human syntaxin 4.

This work was supported by a Jerry and Martha Jarrett Grant for Research on Polycystic Kidney Disease, National Institute of Diabetes and Digestive and Kidney Diseases Grant DK-62338, and Department of Defense Prostate Cancer Research Program Grant DAMD17-02-1-0039.

REFERENCES

1. Al-Awqati Q, Vijayakumar S, Hikita C, Chen J, and Takito J. Phenotypic plasticity in the intercalated cell: the hensin pathway. *Am J Physiol Renal Physiol* 275: F183–F190, 1998.
2. Alper SL, Natale J, Gluck S, Lodish HF, and Brown D. Subtypes of intercalated cells in rat kidney collecting duct defined by antibodies against erythroid band 3 and renal vacuolar H^+ -ATPase. *Proc Natl Acad Sci USA* 86: 5429–5433, 1989.
3. Antonin W, Holroyd C, Tikkanen R, Honing S, and Jahn R. The R-SNARE endobrevin/VAMP-8 mediates homotypic fusion of early endosomes and late endosomes. *Mol Biol Cell* 11: 3289–3298, 2000.
4. Bonilha VL, Marmorstein AD, Cohen-Gould L, and Rodriguez-Boulant E. Apical sorting of influenza hemagglutinin by transcytosis in retinal pigment epithelium. *J Cell Sci* 110: 1717–1727, 1997.
5. Breton S, Inoue T, Knepper MA, and Brown D. Antigen retrieval reveals widespread basolateral expression of syntaxin 3 in renal epithelia. *Am J Physiol Renal Physiol* 282: F523–F529, 2002.
6. Breuza L, Fransen J, and Le Bivic A. Transport and function of syntaxin 3 in human epithelial intestinal cells. *Am J Physiol Cell Physiol* 279: C1239–C1248, 2000.
7. Brown D. Targeting of membrane transporters in renal epithelia: when cell biology meets physiology. *Am J Physiol Renal Physiol* 278: F192–F201, 2000.
8. Brown D, Hirsch S, and Gluck S. An H^+ -ATPase in opposite plasma membrane domains in kidney epithelial cell subpopulations. *Nature* 331: 622–624, 1988.
9. Brown D and Stow JL. Protein trafficking and polarity in kidney epithelium: from cell biology to physiology. *Physiol Rev* 76: 245–297, 1996.
10. Chen YA and Scheller RH. SNARE-mediated membrane fusion. *Nat Rev Mol Cell Biol* 2: 98–106, 2001.
11. Christensen EI, Nielsen S, Moestrup SK, Borre C, Maunsbach AB, de Heer E, Ronco P, Hammond TG, and Verroust P. Segmental distribution of the endocytosis receptor gp330 in renal proximal tubules. *Eur J Cell Biol* 66: 349–364, 1995.
12. Delgrossi MH, Breuza L, Mirre C, Chavrier P, and Le Bivic A. Human syntaxin 3 is localized apically in human intestinal cells. *J Cell Sci* 110: 2207–2214, 1997.
13. Flaumenhaft R, Croce K, Chen E, Furie B, and Furie BC. Proteins of the exocytotic core complex mediate platelet alpha-granule secretion. Roles of vesicle-associated membrane protein, SNAP-23, and syntaxin 4. *J Biol Chem* 274: 2492–2501, 1999.

14. **Fujimoto T and Ogawa K.** Immunoelectron microscopy of fodrin in the rat uriniferous and collecting tubular epithelium. *J Histochem Cytochem* 37: 1345–1352, 1989.
15. **Fujita H, Tuma PL, Finnegan CM, Locco L, and Hubbard AL.** Endogenous syntaxins 2, 3 and 4 exhibit distinct but overlapping patterns of expression at the hepatocyte plasma membrane. *Biochem J* 329: 527–538, 1998.
16. **Gaisano HY, Ghai M, Malkus PN, Sheu L, Bouquillon A, Bennett MK, and Trimble WS.** Distinct cellular locations and protein-protein interactions of the syntaxin family of proteins in rat pancreatic acinar cells. *Mol Biol Cell* 7: 2019–2027, 1996.
17. **Galli T, Zahraoui A, Vaidyanathan VV, Raposo G, Tian JM, Karin M, Niemann H, and Louvard D.** A novel tetanus neurotoxin-insensitive vesicle-associated membrane protein in SNARE complexes of the apical plasma membrane of epithelial cells. *Mol Biol Cell* 9: 1437–1448, 1998.
18. **Grindstaff KK, Yeaman C, Anandasabapathy N, Hsu SC, Rodriguez-Boulant E, Scheller RH, and Nelson WJ.** Sec6/8 complex is recruited to cell-cell contacts and specifies transport vesicle delivery to the basal-lateral membrane in epithelial cells. *Cell* 93: 731–740, 1998.
19. **Hansen NJ, Antonin W, and Edwardson JM.** Identification of SNAREs involved in regulated exocytosis in the pancreatic acinar cell. *J Biol Chem* 274: 22871–22876, 1999.
20. **Hirai Y, Lochter A, Galosy S, Koshida S, Niwa S, and Bissell MJ.** Epimorphin functions as a key morphoregulator for mammary epithelial cells. *J Cell Biol* 140: 159–169, 1998.
21. **Huber LA, Pimplikar S, Parton RG, Virta H, Zerial M, and Simons K.** Rab8, a small GTPase involved in vesicular traffic between the TGN and the basolateral plasma membrane. *J Cell Biol* 123: 35–45, 1993.
22. **Ibaraki K, Horikawa HP, Morita T, Mori H, Sakimura K, Mishina M, Saisu H, and Abe T.** Identification of four different forms of syntaxin 3. *Biochem Biophys Res Commun* 211: 997–1005, 1995.
23. **Ihrke G and Hubbard AL.** Control of vesicle traffic in hepatocytes. *Prog Liver Dis* 13: 63–99, 1995.
24. **Jahn R and Sudhof TC.** Membrane fusion and exocytosis. *Annu Rev Biochem* 68: 863–911, 1999.
25. **Katafuchi K, Mori T, Toshimori K, and Iida H.** Localization of a syntaxin isoform, syntaxin 2, to the acrosomal region of rodent spermatozoa. *Mol Reprod Dev* 57: 375–383, 2000.
26. **Lafont F, Verkade P, Galli T, Wimmer C, Louvard D, and Simons K.** Raft association of SNAP receptors acting in apical trafficking in Madin-Darby canine kidney cells. *Proc Natl Acad Sci USA* 96: 3734–3738, 1999.
27. **Lapierre LA, Tuma PL, Navarre J, Goldenring JR, and Anderson JM.** VAP-33 localizes to both an intracellular vesicle population and with occludin at the tight junction. *J Cell Sci* 112: 3723–3732, 1999.
28. **Lehtonen S, Riento K, Olkkonen VM, and Lehtonen E.** Syntaxin 3 and Munc-18–2 in epithelial cells during kidney development. *Kidney Int* 56: 815–826, 1999.
29. **Lencer WI, Weyer P, Verkman AS, Ausiello DA, and Brown D.** FITC-dextran as a probe for endosome function and localization in kidney. *Am J Physiol Cell Physiol* 258: C309–C317, 1990.
30. **Low SH, Chapin SJ, Weimbs T, Kömüves LG, Bennett MK, and Mostov KE.** Differential localization of syntaxin isoforms in polarized MDCK cells. *Mol Biol Cell* 7: 2007–2018, 1996.
31. **Low SH, Chapin SJ, Wimmer C, Whiteheart SW, Kömüves LK, Mostov KE, and Weimbs T.** The SNARE machinery is involved in apical plasma membrane trafficking in MDCK cells. *J Cell Biol* 141: 1503–1513, 1998.
32. **Low SH, Miura M, Roche PA, Valdez AC, Mostov KE, and Weimbs T.** Intracellular redirection of plasma membrane trafficking after loss of epithelial cell polarity. *Mol Biol Cell* 11: 3045–3060, 2000.
33. **Low SH, Roche PA, Anderson HA, van Ijzendoorn SCD, Zhang M, Mostov KE, and Weimbs T.** Targeting of SNAP-23 and SNAP-25 in polarized epithelial cells. *J Biol Chem* 273: 3422–3430, 1998.
34. **Macaulay SL, Hewish DR, Gough KH, Stoichevska V, MacPherson SF, Jagadish M, and Ward CW.** Functional studies in 3T3L1 cells support a role for SNARE proteins in insulin stimulation of GLUT4 translocation. *Biochem J* 324: 217–224, 1997.
35. **Mandon B, Chou CL, Nielsen S, and Knepper MA.** Syntaxin-4 is localized to the apical plasma membrane of rat renal collecting duct cells: possible role in aquaporin-2 trafficking. *J Clin Invest* 98: 906–913, 1996.
36. **Mandon B, Nielsen S, Kishore BK, and Knepper MA.** Expression of syntaxins in rat kidney. *Am J Physiol Renal Physiol* 273: F718–F730, 1997.
37. **Maranda B, Brown D, Bourgoin S, Casanova JE, Vinay P, Ausiello DA, and Marshansky V.** Intra-endosomal pH-sensitive recruitment of the Arf-nucleotide exchange factor ARNO and Arf6 from cytoplasm to proximal tubule endosomes. *J Biol Chem* 276: 18540–18550, 2001.
38. **McNew JA, Parlati F, Fukuda R, Johnston RJ, Paz K, Paumet F, Sollner TH, and Rothman JE.** Compartmental specificity of cellular membrane fusion encoded in SNARE proteins. *Nature* 407: 153–159, 2000.
39. **Meier KE and Insel PA.** Hormone receptors and response in cultured renal epithelial cell lines. In: *Tissue Culture of Epithelial Cells*, edited by Taub M. New York: Plenum, 1985, p. 145–178.
40. **Min J, Okada S, Kanzaki M, Elmendorf JS, Coker KJ, Ceresa BP, Syu LJ, Noda Y, Saltiel AR, and Pessin JE.** Synip: a novel insulin-regulated syntaxin 4-binding protein mediating GLUT4 translocation in adipocytes. *Mol Cell* 3: 751–760, 1999.
41. **Mostov KE, Verges M, and Altschuler Y.** Membrane traffic in polarized epithelial cells. *Curr Opin Cell Biol* 12: 483–490, 2000.
42. **Moutairou K, Hayez N, Pohl V, Pattyn G, and Pochet R.** Calbindin localization in African giant rat kidney (*Cricetomys gambianus*). *Biochim Biophys Acta* 1313: 187–193, 1996.
43. **Nagamatsu S, Nakamichi Y, Yamamura C, Matsushima S, Watanabe T, Ozawa S, Furukawa H, and Ishida H.** Decreased expression of t-SNARE, syntaxin 1, and SNAP-25 in pancreatic beta-cells is involved in impaired insulin secretion from diabetic GK rat islets: restoration of decreased t-SNARE proteins improves impaired insulin secretion. *Diabetes* 48: 2367–2373, 1999.
44. **Nelson WJ and Yeaman C.** Protein trafficking in the exocytic pathway of polarized epithelial cells. *Trends Cell Biol* 11: 483–486, 2001.
45. **Nielsen S, DiGiovanni SR, Christensen EI, Knepper MA, and Harris HW.** Cellular and subcellular immunolocalization of vasopressin-regulated water channel in rat kidney. *Proc Natl Acad Sci USA* 90: 11663–11667, 1993.
46. **Nielsen S, Terris J, Smith CP, Hediger MA, Ecelbarger CA, and Knepper MA.** Cellular and subcellular localization of the vasopressin-regulated urea transporter in rat kidney. *Proc Natl Acad Sci USA* 93: 5495–5500, 1996.
47. **Obermuller N, Kranzlin B, Blum WF, Gretz N, and Witzgall R.** An endocytosis defect as a possible cause of proteinuria in polycystic kidney disease. *Am J Physiol Renal Physiol* 280: F244–F253, 2001.
48. **Olkkonen VM and Ikonen E.** Genetic defects of intracellular-membrane transport. *N Engl J Med* 343: 1095–1104, 2000.
49. **Olson AL, Knight JB, and Pessin JE.** Syntaxin 4, VAMP2, and/or VAMP3/cellubrevin are functional target membrane and vesicle SNAP receptors for insulin-stimulated GLUT4 translocation in adipocytes. *Mol Cell Biol* 17: 2425–2435, 1997.
50. **Paumet F, Le Mao J, Martin S, Galli T, David B, Blank U, and Roa M.** Soluble NSF attachment protein receptors (SNAREs) in RBL-2H3 mast cells: functional role of syntaxin 4 in exocytosis and identification of a vesicle-associated membrane protein 8-containing secretory compartment. *J Immunol* 164: 5850–5857, 2000.
51. **Peng SB, Crider BP, Tsai SJ, Xie XS, and Stone DK.** Identification of a 14-kDa subunit associated with the catalytic sector of clathrin-coated vesicle H⁺-ATPase. *J Biol Chem* 271: 3324–3327, 1996.
52. **Pollack AL, Runyan RB, and Mostov KE.** Morphogenetic mechanisms of epithelial tubulogenesis: MDCK cell polarity is transiently rearranged without loss of cell-cell contact during

- scatter factor/hepatocyte growth factor-induced tubulogenesis. *Dev Biol* 204: 64-79, 1998.
53. **Quinones B, Riento K, Olkkonen VM, Hardy S, and Bennett MK.** Syntaxin 2 splice variants exhibit differential expression patterns, biochemical properties and subcellular localizations. *J Cell Sci* 112: 4291-4304, 1999.
 54. **Riento K, Galli T, Jansson S, Ehnholm C, Lehtonen E, and Olkkonen VM.** Interaction of munc-18-2 with syntaxin 3 controls the association of apical SNAREs in epithelial cells. *J Cell Sci* 111: 2681-2688, 1998.
 55. **Rodger J, Davis S, Laroche S, Mallet J, and Hicks A.** Induction of long-term potentiation in vivo regulates alternate splicing to alter syntaxin 3 isoform expression in rat dentate gyrus. *J Neurochem* 71: 666-675, 1998.
 56. **Scales SJ, Chen YA, Yoo BY, Patel SM, Doung YC, and Scheller RH.** SNAREs contribute to the specificity of membrane fusion. *Neuron* 26: 457-464, 2000.
 57. **Snider MD and Rogers OC.** Membrane traffic in animal cells: cellular glycoproteins return to the site of Golgi mannosidase I. *J Cell Biol* 103: 265-275, 1986.
 58. **Steegmaier M, Lee KC, Prekeris R, and Scheller RH.** SNARE protein trafficking in polarized MDCK cells. *Traffic* 1: 553-560, 2000.
 59. **Steinman RM, Mellman IS, Muller WA, and Cohn ZA.** Endocytosis and the recycling of plasma membrane. *J Cell Biol* 96: 1-27, 1983.
 60. **Tellam JT, Macaulay SL, McIntosh S, Hewish DR, Ward CW, and James DE.** Characterization of Munc-18c and syntaxin-4 in 3T3-L1 adipocytes. Putative role in insulin-dependent movement of GLUT-4. *J Biol Chem* 272: 6179-6186, 1997.
 61. **Weber E, Berta G, Tousson A, St. John P, Green MW, Gopalokrishnan U, Jilling T, Sorscher EJ, Elton TS, Abrahamson DR, and Kirk KL.** Expression and polarized targeting of a rab3 isoform in epithelial cells. *J Cell Biol* 125: 583-594, 1994.
 62. **Weimbs T, Low SH, Chapin SJ, and Mostov KE.** Apical targeting in polarized epithelial cells: there's more afloat than rafts. *Trends Cell Biol* 7: 393-399, 1997.
 63. **Yang C, Coker KJ, Kim JK, Mora S, Thurmond DC, Davis AC, Yang B, Williamson RA, Shulman GI, and Pessin JE.** Syntaxin 4 heterozygous knockout mice develop muscle insulin resistance. *J Clin Invest* 107: 1311-1318, 2001.
 64. **Zahraoui A, Joberty G, Arpin M, Fontaine JJ, Hellio R, Tavitian A, and Louvard D.** A small rab GTPase is distributed in cytoplasmic vesicles in non polarized cells but colocalizes with the tight junction marker ZO-1 in polarized epithelial cells. *J Cell Biol* 124: 101-115, 1994.
 65. **Zolotnitskaya A and Satlin LM.** Developmental expression of ROMK in rat kidney. *Am J Physiol Renal Physiol* 276: F825-F836, 1999.
 66. **Zurzolo C, Le Bivic A, Quaroni A, Nitsch L, and Rodriguez-Boulan E.** Modulation of transcytotic and direct targeting pathways in a polarized thyroid cell line. *Embo J* 11: 2337-2344, 1992.

